Nuclear Quadrupole Interactions as a Probe of Glass Molecular Structure *

P. Boolchand

Department of Electrical Engineering and Computer Science, University of Cincinnati, Cincinnati, OH 45221-0030, USA

Z. Naturforsch. **51a**, 572–584 (1996); received October 20, 1995

^{125}Te absorption and ^{129}I emission Mössbauer spectroscopies have proved to be the methods of choice to probe chalcogen chemical order in condensed matter using nuclear quadrupole interactions. In chalcogenide glasses, the technique has been unusually rewarding in decoding both the elements of local atomic structures and those of the medium-range atomic structures.

Introduction

Chalcogens (S, Se and Te) display a rich variety of oxidation states and chemical bonding configurations in inorganic solids. For example, take the case of Te for which oxidation states of 2^-, 0, 2^+, 4^+ and 6^+ are not uncommon in crystalline compounds. The ionic radius in each of these oxidation states is different, and in crystalline solids it is usually always possible to establish details of crystallographic structure, including local atomic coordination by X-ray diffraction and/or neutron Bragg scattering. In disordered materials such as amorphous solids and glasses, on the other hand, these traditional structural methods, although necessary, are found to be inadequate to establish the details of glass structure [1], in spite of new developments in the field. In disordered materials, nuclear quadrupole interactions (NQI) have proved to be particularly successful as probe of local structure. This is largely the case because the open "p" shell in the chalcogens usually results in a large valence contribution to the local electric field gradient (EFG) which is correlated to local bonding configurations [2]. In principle, EFGs can be established by traditional methods used to study NQI in solids. However, nuclear quadrupole resonance (NQR) spectroscopy using a nuclear ground state cannot be used because neither Se nor Te have probe nuclei that possess a finite quadrupole moment (Q) in the ground state. In fact, in the group VI elements the only NQR probes of interest include ^{33}S (nat. abund. 0.76%) and ^{17}O (nat. abund. 0.0376%). The minuscule natural abundances of these isotopes, understandably, has restricted applications [3] of these NQR probes.

The lack of NQR probes in the chalcogens had been a challenge up until three decades ago. This challenge also opened new opportunities then. The discovery of the Mössbauer effect in ^{125}Te [4] and ^{129}I [5] in the early sixties made accessible nuclear quadrupole effects using the first exicited state ($3/2^-$) at 35.5 keV in ^{125}Te and both the ground and first excited state in ^{129}I. In spite of the intrinsically wide natural-width (5.2 mm/s) of the ^{125}Te nuclear-resonance, from experiments performed over the years it has emerged [5] as an extremely useful probe of Te local environments and chemistry in a wide array of chalcogen-based materials. There are four outstanding reasons. First, Te quadrupolar effects are indeed quite large, leading in many instances to quadrupole splittings ($\Delta \simeq e^2 q Q/2 \simeq 10$ mm/s) that exceed the natural linewidth of the gamma resonance and result in partially resolved doublets in the observed lineshapes. Second, the lineshape centroid, measured with respect to a standard host, also known as the isomer shift, provides directly the Te oxidation state (Figure 1). These shifts span a range of 3 mm/s, representing 60% of the natural width. Third, ^{125}Te Mössbauer methodology has evolved to the point that spectra of Te compounds can now be taken with a source at room temperature [7], as is routinely done with the more popular resonances in ^{57}Fe and ^{119}Sn. Fourth, and perhaps the key to the success of this method, it has been the recognized that NQI parameters deduced from ^{125}Te absorption spectroscopy are quantitatively correlated to those from ^{129}I emission Mössbauer spectroscopy when the par-

* Presented at the XIIIth International Symposium on Nuclear Quadrupole Interactions, Providence, Rhode Island, USA, July 23–28, 1995.

Reprint requests to Prof. Dr. P. Boolchand.

0932-0784 / 96 / 0500-0572 $ 06.00 © – Verlag der Zeitschrift für Naturforschung, D-72072 Tübingen

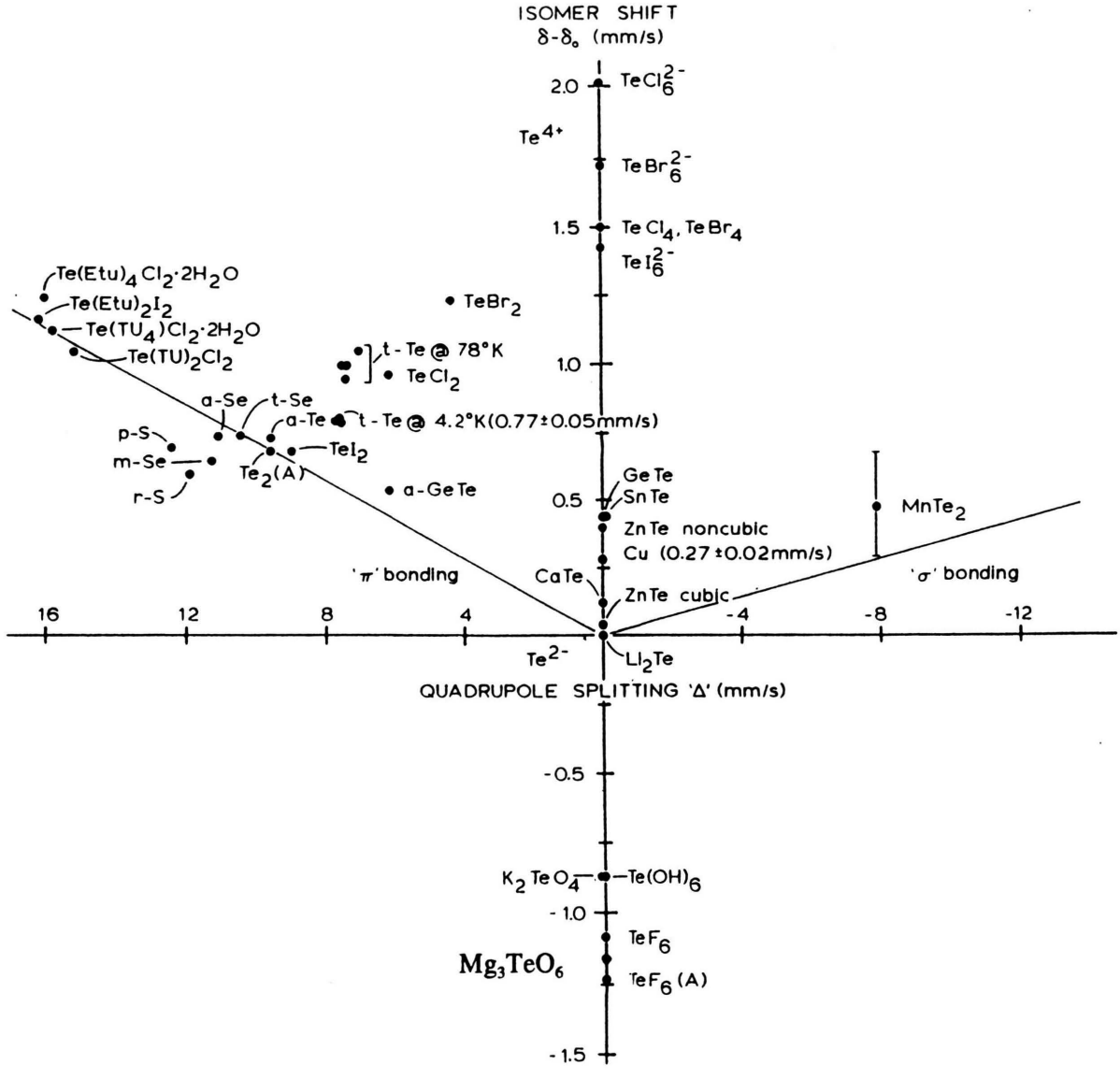

Fig. 1. ^{125}Te isomer shifts δ (mm/s) quadrupole splittings (mm/s) in inorganic Te compounds. The shifts are relative to Li_2Te corresponding to the Te^{2-} closed shell configuration. See text for details

ent Te-site is 2-fold coordinated. In the latter spectroscopy one dopes the same Te (chalcogen) host material of interest with traces of ^{129m}Te and measures the NQI at the daughter ^{129}I site formed from β-decay of the ^{129m}Te parent. The narrow natural-width (0.59 mm/s), favorable spin-sequence $5/2^+ \rightarrow 7/2^+$, and large nuclear quadrupole moments associated with both the ground ($7/2^+$) and excited ($5/2^+$) state of the 27.7 keV γ-resonance, makes directly accessible the magnitude, sign and asymmetry parameter η of the ^{129}I EFG even in a polycrystalline sample. Furthermore, because of a change in chemical valence from a Te parent to an I daughter, in most cases considerable simplification occurs in the possible I-sites formed upon nuclear transmutation. Indeed, the quantitative correlations between the ^{125}Te and ^{129}I NQI parameters in crys-

talline solids have added a good measure of confidence in parent Te-site assignments. In glasses where bimodal [8] and trimodal [9] distribution of Te sites has been observed, these site distributions have provided crucial insight in decoding the molecular structure of chalcogenide and chalcohalide glasses.

Electric Field Gradient Sign Reversal From Te to I in Elemental Chalcogens

The elemental chalcogens crystallize in phases consisting of chains or rings in which the hallmark of chemical bonding is a low coordination number (cn) of 2. For a chalcogen atom (6 valence electrons, $s^2 p^4$), a cn of 2 is realized with two of the p electrons entering in covalent bonds with their two next nearest neighbors (nns), and the remaining two electrons forming non-bonding lone-pairs, schematically illustrated in Figure 2.

This distribution of electrons gives rise to a valence contribution to the Te EFG which is negative and is due to one p_z electron, i.e. $= -(4/5)(I^{el}/\langle r^3\rangle)$. Since the nuclear quadrupole moment ($Q = -0.31$ b) of the 35.5 keV state in ^{125}Te is negative [10], the sign of the quadrupole coupling $e^2 Q q$ in a 2-fold coordinated host, such as crystalline Te, is expected to be positive, i.e. the quadrupole splitting in the $I = 3/2$ state leaves the $m_I = \pm 3/2$ sublevels at a higher energy than the $m_I = \pm 1/2$ sublevels, as was confirmed by Mössbauer spectroscopy measurements on Te single-crystals [11] many years back.

^{129}I emission spectra of crystalline Te reveal the quadrupole coupling to possess a negative sign [12]. Since the ground state quadrupole moment of ^{129}I nuclei is negative, one must infer that the ^{129}I EFG possesses a positive sign in crystalline Te. The sign reversal in the EFG from a Te-parent (negative) to an I-daughter (positive) is ascribed [13] to a two-fold coordinated Te-parent site leading to a nominally one-fold coordinated I-daughter site. Apparently, the monovalent I-atom breaks a bond with one of its Te neighbors and σ-bonds to the other Te nearest neighbor (Figure 2). The positive sign of the ^{129}I EFG is then ascribed to σ-bonding due to a p_z hole ($+4/5\,|e|/\langle r^3\rangle$) as for example in a diatomic I_2 molecule. The sign change in the EFG from negative at Te to positive at I, when the parent Te atom is 2-fold coordinated, has also been observed [12] for the Te atom as an impurity in the various polymorphs of elemental Se and also those of S. Indeed this pattern of a negative ^{129}I quadrupole coupling whenever the parent ^{129m}Te site is 2-fold coordinated, has been observed universally. Furthermore, whenever the Te parent has a cn greater than 2, the ^{129}I EFG retains the positive sign of the Te parent. These trends have been extremely useful to establish the Te parent cn in glasses, as we shall illustrate with specific examples.

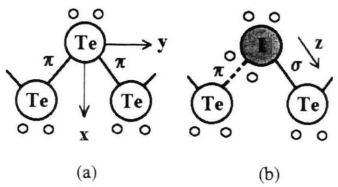

Fig. 2. (a) V_{zz} component of the EFG tensor for a 2-fold coordinated Te atom as in c-Te, directed perpendicular to the Te–Te–Te plane. (b) Upon β-decay of ^{129}Te parent, the ^{129}I daughter formed becomes σ bonded to one of the Te nearest-neighbor atoms and the V_{zz} component of the EFG is now directed along the bond. The small circles designate lone pair electrons.

Correlation between ^{125}Te and ^{129}I Nuclear Quadrupole Couplings

In chalcogen-bearing molecular crystals, it is possible to quantitatively correlate the ^{125}Te EFG with the ^{129}I EFG following the Townes-Daily [14] formalism when the chalcogen is 2-fold coordinated. In such crystals one defines the imbalance in the p charge density U_p as the ratio of the observed nuclear quadrupole coupling to the atomic quadrupole coupling, i.e. $(e^2 q Q)_{obs} = U_p (e^2 q Q)$. Quantitatively, the ratio R of ^{125}Te to ^{129}I nuclear quadrupole couplings can then be written as

$$R = \frac{U_p(\text{Te})\, e^2 q(\text{Te-atom})\, Q(^{125}\text{Te})}{U_p(\text{I})\, e^2 q(\text{I-atom})\, Q(^{129}\text{I})}. \qquad (1)$$

Taking $Q(^{125}\text{Te}) = -0.31$ b, $Q(^{129}\text{I}(7/2)) = -0.55$ b, $eq(\text{Te-atom}) = 15.0$ atomic units [15] and $eq(\text{I-atom}) = 18.0$ atomic units [15], the ratio R is found to be -0.48 for the case when $U_p(\text{Te}) = -U_p(\text{I})$, as it would be when the parent Te is 2-fold coordinated and the daughter I 1-fold. This calculation is applicable in hosts when the valence contribution to the EFG far exceeds the lattice contribution to the EFG. This is the case in molecular solids [13] like plastic S or rhombic S or the Te-thiourea complexes [10]. As the lattice contribution ot the EFG becomes increasingly important, this ratio systematically decreases [13] from -0.48 in

rhombic S, to -0.65 in trigonal Se, to -1.12 in trigonal Te. We have suggested [13] that this is largely because the lattice contribution to the EFG at a substitutional site in the trigonal chains of Se and Te has a negative sign [16], so that numerically the valence and lattice contributions to the EFG at a Te site add in the numerator, while these contributions being of opposite sign at an I site, subtract in the denominator of the equation

$$R = \frac{e\,Q(^{125}\mathrm{Te})[V_{zz}^{\mathrm{val}}(\mathrm{Te}) + V_{zz}(\mathrm{lat})]}{e\,Q(^{129}\mathrm{I})[V_{zz}^{\mathrm{val}}(\mathrm{I}) + V_{zz}(\mathrm{lat})]}. \tag{2}$$

Correlation of ^{129}I Isomer-shifts with Nuclear Quadrupole Couplings

The centroid of the nuclear resonance lineshape in ^{129}I Mössbauer spectroscopy, measured relative to a standard host such as CuI^{129}, yields the isomer shift. Emperically, this shift has been shown [12] to be given by

$$\delta = -(9 \pm 1)\,h_s + (1.5 \pm 0.1)\,h_p - (0.13 \pm 0.02)\ \mathrm{mm/s}, \tag{3}$$

where h_s and h_p designate the number of s and p holes, i.e. $h_s = 2 - n_s$ and $h_p = 6 - n_p$, n_s and n_p being the number of 5 s and 5 p electron on I. When I displays pure σ-bonding, as in an I_2 molecule, then the shift can be related to the nuclear quadrupole coupling. For the case when $\eta = 0$, one can show [12] that

$$\delta - \delta_0 = 1.5\,e^2\,q\,Q(\mathrm{Mhz})/1608, \tag{4}$$

(4) describing the "σ" line drawn at 45° to the $+x$ axis in Figure 3. When I displays pure π-bonding as in BiI_3 [17], the corresponding relation is given by

$$\delta - \delta_0 = 3.0\,e^2\,q\,Q(\mathrm{Mhz})/1608, \tag{5}$$

and (5) represents the "π" line drawn at 135° to the $+x$ axis in Figure 3. In the figure data points corresponding to various I-compounds reside between the π- and σ-line in the top half of the plot. Departures away from the pure "σ" line are indication of some "π" bonding admixture, and vice-versa. In the plot, note that there are no points that lie in the 3rd and 4th quadrant, except those that reside along the $-y$ axis for which $e^2\,q\,Q \to 0$.

Correlation of ^{125}Te Isomer-shift with Nuclear Quadrupole Couplings

Figure 1 displays a plot of ^{125}Te isomer-shifts versus quadrupole couplings for several inorganic Te compounds. An empirical relation parallel to (3) can be written for the ^{125}Te nuclear resonance as

$$\delta = -2.6\,h_s + 0.43\,h_p - 0.15\ \mathrm{mm/s} \tag{6}$$

by normalizing [18] for the nuclear charge radius change $\delta\langle r^2\rangle$ between the ^{125}Te and ^{129}I resonances. Relations parallel to those of (4) and (5) can be written for ^{125}Te, taking $e\,q$(Te) to be 19.2 mm/s. On this plot all shifts are quoted relative to Te^{2-}, i.e. $s^2\,p^6$ closed shell configuration in analogy to I^-, i.e. $s^2\,p^6$ for the case of ^{129}I. Unlike the case of ^{129}I, where the majority of I-compounds display σ bonding yielding a negative $e^2\,q\,Q$, in the case of ^{125}Te one encounters Te compounds displaying primarily π-bonding with a positive $e^2\,q\,Q$.

Molecular Structure of Binary Chalcogenide Glasses

Binary alloys of As and Ge with the chalcogens S and Se, but not Te, form melt-quenched $As_x(S\text{ or }Se)_{1-x}$ and $Ge_y(S\text{ or }Se)_{1-y}$ bulk glasses over a wide composition range $0 < x < 0.45$ and $0 < y < 0.43$. The molecular structure of the stoichiometric glasses at $x = 0.4$, i.e. As_2S_3 or As_2Se_3, and at $y = 0.33$, i.e. GeS_2 or $GeSe_2$ has been the subject of numerous studies by a variety of methods including X-ray or neutron scattering [19], extended X-ray absorption fine structure (EXAFS) [20], ^{75}As NQR [21], Raman scattering [22] IR reflectance [23], molecular dynamic simulations [24] and thermal methods such as scanning calorimetry [25].

There is broad recognition that the basic building blocks of these glassy networks at stoichiometric compositions, in analogy to their crystalline counterparts, consist of pyramidal units: $As(S_{1/2})_3$ or $As(Se_{1/2})_3$, or tetrahedral units $Ge(S_{1/2})_4$ or $Ge(Se_{1/2})_4$, as the case may be. In the high-temperature crystalline phase [26, 27], these building blocks form fully polymerized layered (2 d) structures with layers separated by a van der Waals gap, due to lone-pair repulsion. In corresponding glasses, some have argued that the networks are also fully polymerized but intstead possess a 3 d morphology, in analogy to the case of SiO_2 glass as advanced by Zachariasen in the celebrated paper [28] of 1932. The term often used to describe this structure is

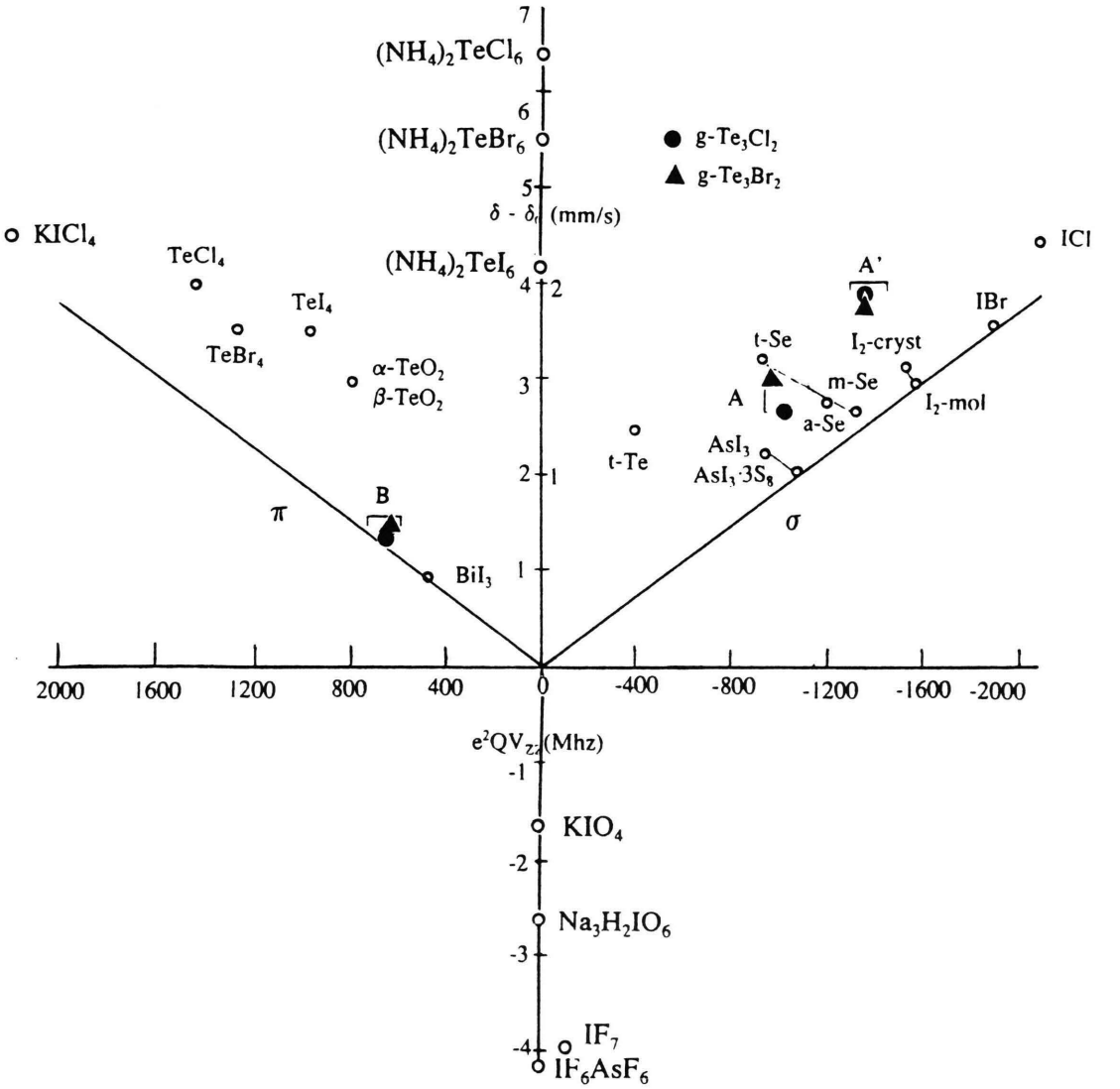

Fig. 3. ^{129}I isomer-shifts δ(mm/s) versus quadrupole couplings (in Mhz) in selected Te-compounds used as sources and selected I-compounds used as absorbers. See text for details.

"chemically ordered continuous random network" (COCRN), An alternative model, advocated by J. C. Phillips, visualized these stoichiometric glasses to consist [29, 30] of electron-rich, large, partially polymerized crystal-like molecular clusters and electron-deficient, small molecular fragments. In this microcrystalline model the electron-rich clusters are thought to be bordered by S–S or Se–Se dimers thus defining an internal surface, while the electron-deficient smaller fragments have compensating Ge–Ge or As–As bonds in the form of ethane-like $(Ge_2Se_3)_n$ or As_4Se_4 monomeric or polymeric fragments. In the latter model, some degree of molecular phase separation is thought to be intrinsic to the glassy state and serves to provide a barrier towards crystallization.

g-$GeSe_2$ and g-GeS_2

A continuous random network of corner sharing $Ge(Se_{1/2})_4$ or $Ge(S_{1/2})_4$ tetrahedra would result in one type of a chalcogen site. This is a bridging site having two Ge nearest-neighbors (nn) that would be common

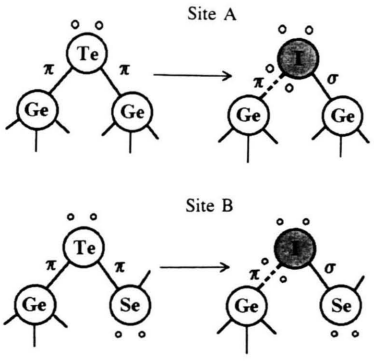

Fig. 4. Expected parent Te-sites (on left) and resulting daughter I (on right) when ^{129m}Te dopant atoms substitute Se sites in a $GeSe_2$ glass. For a chemically ordered continuous random network only site A (I–Ge) is expected to be observed. Presence of some Se–Se bonds in the $GeSe_2$ glass network will give rise to some site B (I–Se) to be populated. See text for details.

to both g-$GeSe_2$ and g-GeS_2 networks. Te as a dopant in these glasses would be expected to substitute for Se and S and thus form a site with two Ge nearest-neighbors, henceforth denoted as site A: the chemically ordered site. On the other hand, if the random network possessed some heteropolar bonds, Se–Se and Ge–Ge bonds as the principal defects, then one expects the chalcogen dimers to give rise to some chalcogen sites having a Ge and a chalcogen nearest-neighbor. This would lead to some Te dopant sites having a Ge and a Se(or S) nearest neighbor (see Fig. 4), henceforth denoted as site B: the chemically disordered site.

The resulting daughter ^{129}I site, formed from ^{129m}Te doping of g-$GeSe_2$ from site A, is expected (see Fig. 4) to be a one-fold coordinated I-site σ-bonded to one of two Ge nearest neighbors. For site B, the daughter ^{129}I site is also expected to be onefold coordinated, but it will be σ-bonded to the Se(S) nearest-neighbor and not to the Ge-neighbor. This is largely the case because the lone pair repulsive (non-bonding) interactions between an I and Se(S) atom overwhelm the charge transfer effects. We must remember that these bonds are formed in the solid glassy network and not in the vapor phase. Because of van der Waals interactions, I will form a σ bond with the Se(S) nearest-neighbor atom even though such bonding does not optimize charge transfer effects.

^{129}I emission spectra of g-$GeSe_2$ (and also g-GeS_2) do indeed reveal [8] (Fig. 5) a bimodal distribution of I sites: the chemically ordered site A (I-Ge) and the chemically disordered site B (I-Se). The widely differ-

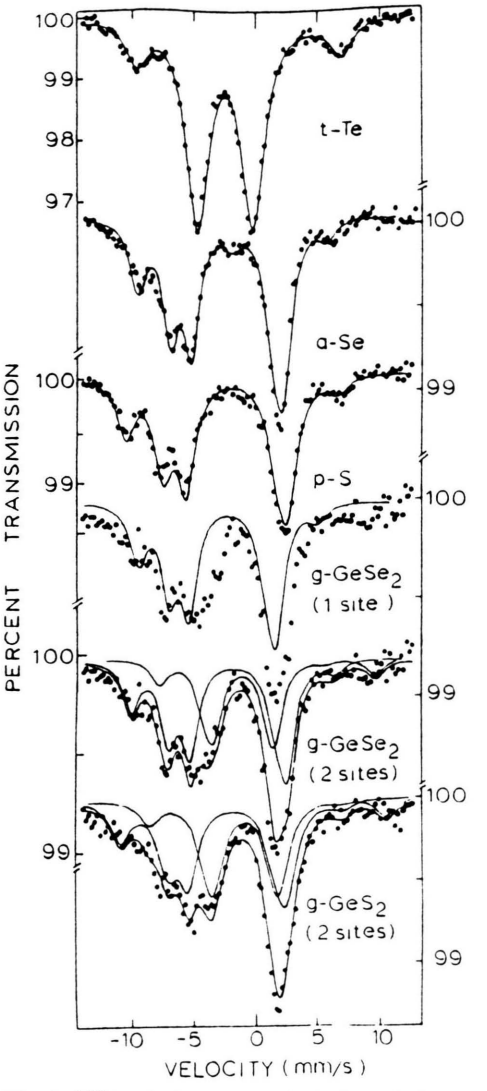

Fig. 5. ^{129}I emission spectra in indicated elemental chalcogens and $GeSe_2$ and GeS_2 glass taken from [8]. A qualitative improvement in the $GeSe_2$ glass spectrum results in going from a 1-site fit to a 2-site fit. Further, one of the sites observed in GeS_2 and $GeSe_2$ glass is characterized by the same electric quadrupole interaction parameters and is identified with site A: I "σ" bonded to a Ge nn.

ent quadrupole couplings of these sites lead to a well resolved hyperfine structure. Surprisingly, the experimental results also show that the site intensity ratio I_B/I_A is 1.6, i.e. the defect site is more strongly populated than the chemically ordered site in these glasses.

The surprising site populations, viz., $I_B > I_A$ in these glasses, constitutes direct evidence [8] for the chemical

bond reconstruction (Se–Se, S–S) on cluster-surfaces alluded to by J. C. Phillips [29]. The oversized Te-dopant apparently segregates to cluster surfaces selectively replacing Se at B-sites rather than the cluster interior A-site. Such segregation is driven by strain energy considerations: Te for Se substitution at B-sites on cluster surfaces permits the oversized dopant to relax in the van der Waals gap. Such a strain relief mechanism is precluded for Te substitution at A-sites in the cluster interior.

^{129}I Mössbauer spectroscopy measurements of the site-intensity ratios I_B/I_A as a function of glass composition "x" in the $GeSe_{2-x}Te_x$ ternary has revealed a power-law variation (Figure 6). We have modeled [8] the glass network to be composed of Ge–Se–Ge and Ge–Se–Se–Ge strings, and have used tools of statistical mechanics to fit the observed $I_B/I_A(x)$ variation in terms of two parameters, β and ϱ. The β-parameter physically relates to Te dopant selectivity of B over A sites, while the ϱ-parameter gives the stoichiometry of the Se-rich cluster, i.e. $Ge:Se = 1:2(1+2\varrho)/(1+\varrho)$. A finite value of ϱ implies a Se-rich cluster. The results reveal that a value of $\beta \gtrsim 13$ and a value of $\varrho \leq 1/16$ would provide a reasonable description of the observed $I_B/I_A(x)$ trend over the composition range $0 < x < 0.20$. These results directly imply that in g-$GeSe_2$, Te dopant prefers B-sites over A-sites by at least a factor of 13. Furthermore, as shown elsewhere [6, 8], the value of $\varrho \leq 1/16$ suggests the degree of broken cation chemical order, i.e. the concentration ratio of chemically disordered Ge sites to the concentration of available ordered and disordered Ge sites, i.e. $N_B/(N_A+N_B)$ of the network to be 0.16(3).

In a stoichiometric $GeSe_2$ or GeS_2 glass, the presence of a finite concentration of Se–Se or S–S bonds would require an equivalent concentration of Ge–Ge bonds to appear in the network. In the molecular phase separation model of these glasses, the Ge–Ge bonds form the backbone of an ethane-like molecular fragment. Thus two types of Ge sites are expected to occur: Site A, a chemically ordered Ge site tetrahedrally coordinated to 4 Se or S nearest-neighbors and site B, a chemically disordered Ge site having three Se and on Ge nns. In this model of molecular phase separation, Ge site A becomes the signature of the Se-rich cluster while the Ge site B that of the Ge-rich cluster. ^{119}Sn Mössbauer spectroscopy (Fig. 7) provides an elegant means to establish the details of Ge chemical order in these glasses since Sn is isovalent to Ge and as a dopant can be expected to replace available Ge

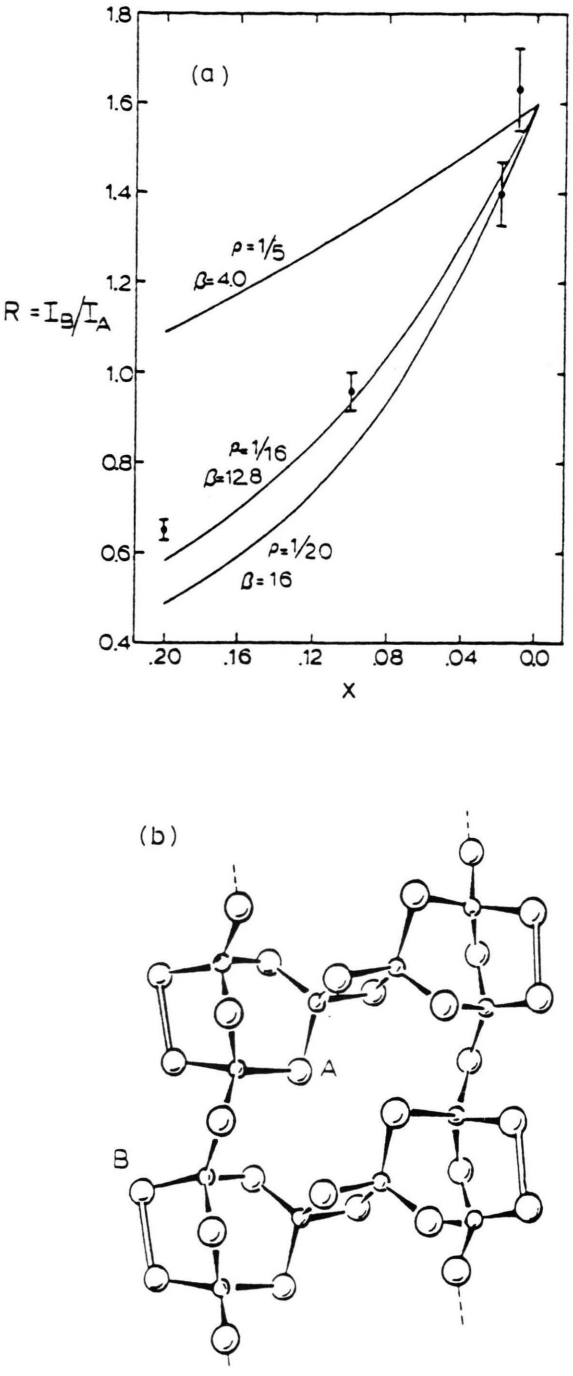

Fig. 6. (a) Observed variation of ^{129}I Mössbauer site intensity ratio a $I_B/I_A(x)$ in $GeSe_{2-x}Te_x$ glasses displaying a power law behavior as $x \to 0$, [8]. (b) Molecular fragment of the layer form of c-$GeSe_2$ with edges reconstructed to form Se–Se dimers [29]. The dopant selects the outrigger Se sites (B) of the dimers over the bridging Se sites (A) in the cluster interior as revealed by I_B/I_A in the Mössbauer spectroscopy results, [8].

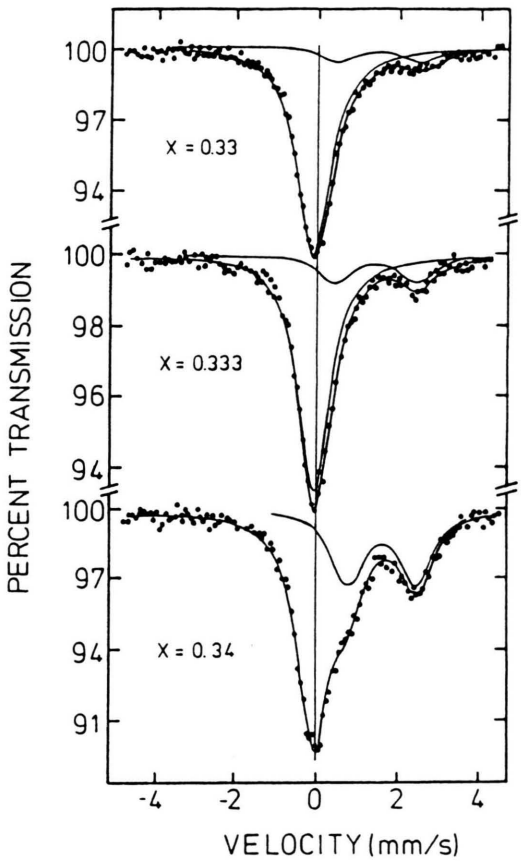

Fig. 7. ^{119}Sn spectra of indicated $(Ge_{0.99}Sn_{0.01})_xSe_{1-x}$ glasses showing presence of two sites at $x=1/3$, a tetrahedral site (site A) contributing to the narrow resonance at $v=0$ mm/s and a non-tetrahedral site (site B) displaying a quadrupole doublet, [31].

cation sites of the network. Such Mössbauer spectroscopy experiments were undertaken [31] on bulk $(Ge_{0.99}Sn_{0.01})_xSe_{1-x}$ glasses doped with isotopically enriched ^{119}Sn. The results reveal that at $x=1/3$, two ^{119}Sn (A, B) sites occur in the network with the ratio $I_B/(I_A+I_B)=0.16$, in harmony with the ^{129}I Mössbauer spectroscopy results. Thus, both cationic and anionic probes of glass structure independently yield the same details on the degree of broken chemical order in stoichiometric $GeSe_2$ glass. The structural model of this glass based on an intrinsic molecular phase separation into chalcogen-rich and Ge-rich clusters is consistent with Mössbauer spectroscopy results. Recent Raman [32] scattering and neutron scattering [33] results on $GeSe_2$ glass lend further support for such a model.

Finally, it would be appropriate to remember that the present ^{129}I Mössbauer spectroscopy results could not be understood even qualitatively in terms of a COCRN as a model description of $GeSe_2$ or GeS_2 glass. In such a model, one visualizes a 3d-network to consist predominantly of the chemically ordered A-sites, with the chemically disordered sites (site B) formed at random as point defects. In such a homogeneous micro-morphology, one expectes Te dopant to *randomly* replace available A- and B-sites, yielding $\beta\sim 1$ and $I_B/I_A\sim 0.10$. These expectations are qualitatively incompatible with the observed site selectivity $\beta\geq 13$ and Mössbauer site intensity ratio of $I_B/I_A=1.6$.

g-As_2Se_3 and g-As_2S_3

In 1979, as constraint theory [34, 35, 36] of glasses evolved, one came to recognize that $As(S_{1/2})_3$ or $As(Se_{1/2})_3$ pyramidal units that form building blocks of As_2Se_3 and As_2S_3 glasses are rather special. Specifically, if one enumerates bond-stretching and bond-bending constraints per atom for a pyramidal unit, one finds that there are on an average three constraints/atom. And since there are three degree of freedom associated with each atom, several interesting consequences follow from the exact balance of constraints/atom with degrees of freedom. Some of these consequences include (a) that the glass forming tendency in the As_xSe_{1-x} and As_xS_{1-x} binary glass system are optimized at $x=2/5$, when the network consists largely of pyramidal building blocks, (b) that as pyramidal units sit at a mechanical critical point, they can easily distort about their mean position with little expense in strain energy to form a continuous network, (c) that one consequence of (b) is that bond-angles and bond-lengths in As_2Se_3 glass network will in general display a larger spread than the spread displayed by the more constrained tetrahedral units in a $GeSe_2$ glass network and finally, (d) for this latter reason, Raman vibrational modes in As_2Se_3 glass [37] are found to display broad bands rather than the narrow ones encountered in the more constrained $GeSe_2$ glass.

One of the first applications of ^{75}As NQR spectroscopy to probe glass structure was to As_2S_3 and As_2Se_3 glasses. The ^{75}As nuclear quadrupole couplings in both these glasses revealed [21], not unexpectedly, broad distribution in contrast to sharply defined couplings in corresponding crystals. Noteworthy in the

NQR results were the facts that (a) the nuclear quadrupole couplings in the glasses were centered around the corresponding crystalline site parameters of orpiment (c-As_2S_3) and c-As_2Se_3, and (b) the transverse spin-spin relaxation times in the glasses and corresponding crystal were nearly the same. These results provided the first clue that the molecular structure of these glasses bears a close connection to that of the corresponding layered crystals. Szeftel and Allou [38] measured the asymmetry parameter (η) of the EFG at As sites in the glasses by a magnetic perturbation of the nuclear quadrupole interaction. In both glasses these authors found that the η distribution could be deconvoluted in terms of two Gaussians. In g-As_2S_3 for example, the Gaussian with the larger weight (60%) was characterized by an almost axially symmetry EFG, i.e. $\eta_{1m}=0.12(2)$, while the second Gaussian with a smaller weight (40%) was characterized by a larger asymmetry parameter $\eta_{2m}=0.36$. Parallel results were found in g-As_2Se_3, where $\eta_{1m}=0.14(2)$ and $\eta_{2m}=0.45$.

In the crystal structure of orpiment, two chemically inequivalent As sites (As_I and As_{II}) occur with equal frequency in the 2d layers. The measured [21] quadrupole coupling constants at 4.2 K of As_I of 72.9 Mhz and asymmetry parameter $\eta=0.343$, and of As_{II} of 70.4 Mhz and asymmetry parameter $\eta_2=0.374$ can be qualitatively understood in terms of a valence contribution to the EFG as discussed by Rubinstein and Taylor. In fact the simplistic estimates of the asymmetry parameters for these sites based entirely on intrapyramidal hybridized orbitals gave values of $\eta_1=0.15$ and $\eta_2=0.42$, which are surprisingly close to the mean values of the two Gaussian distributions reported by Szeftel in the glasses. Thus a likely interpretation of the η-values in the glasses, reported by Szeftel [38], is that these are actually characteristic of the local pyramidal units and are emphasized in the glass, while the η values observed in the crystalline phases include the effect of long-range order as well.

Perhaps a more stringent test of the structural models of As_2Se_3 glass (Fig. 8) has emerged from the ^{129}I and ^{125}Te Mössbauer spectroscopy measurements. Specifically, these measurements provide direct evidence for the edge-reconstruction of As_6Se_6 puckered rings (Fig. 8) leading to an intrinsic phase separation of the stoichiometric glass into Se-rich and As-rich clusters advanced by J.C. Phillips [30]. Such Mössbauer spectroscopy measurements in the

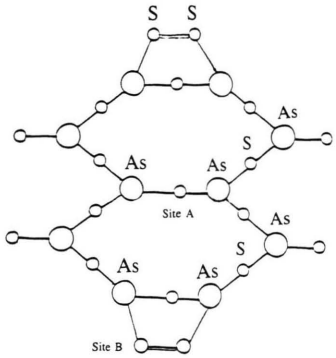

Fig. 8. Molecular structure of As_2S_3 glass consisting of 12 membered As_6S_6 rings bordered by S–S dimers proposed by J.C. Phillips, [30]. Within this orpimental raft model a smaller concentration of S–S bonds in the network can exist if the edge reconstruction occurs between multiple-rings. ^{129}Te dopant occupancy at the chemically disordered outrigger sites (B) over the chemically ordered intraring sites (A) appears to be driven by the larger Te dopant size in relation to the host chalcogen (S) size.

$As_2Se_{3-x}Te_x$ glass system were undertaken [38] over the entire composition range $0<x<3$. Clear evidence of a bimodal distribution of ^{129}I sites (A, B) resulting from 2-fold coordinated parent Te-sites emerged as $x\to 0$. As in the case of $GeSe_{2-y}Te_y$ glasses, in $As_2Se_{3-x}Te_x$ glasses, one also found a power-law variation of the site-intensity ratio $I_B/I_A(x)$ with Te-concentration "x" (or "y") with a ratio of 1.6 at $x\simeq 0.0033$ (Fig. 9), to account for the power-law variation of $I_B/I_A(x)$, Suranyi et al. [39] developed a model of these glasses starting from the premise that the network is largely composed of single-chalcogen-bearing As–Se–As strings and double-chalcogen-bearing As–Se–Se–As strings in which Te dopand substitutes available Se-sites. To account for the observed power-law variation of $I_B/I_A(x)$ in the range $0<x<0.20$, Suranyi et al. [40] found necessary to require Te dopant sites to select the chemically disordered sites (B-sites) over the chemically ordered ones (A-sites) by a factor of at least 36, and the Se-rich cluster to possess a stoichiometry $As:Se=2:3(1+2\varrho)/(1+\varrho)$ with $\varrho\leq 1/40$. The latter result suggests a Se-rich cluster consisting of about 15-rings of As_6Se_6 whose edges have been reconstructed by Se–Se dimers. One is thus led to the conclusion that the size of the Se-rich cluster in As_2Se_3 glass is larger than in $GeSe_2$ glass. In particular the degree of broken cation chemical order in As_2Se_3 glass is predicted to be about 7%, which is a factor of 2 smaller than in $GeSe_2$ glass (14%).

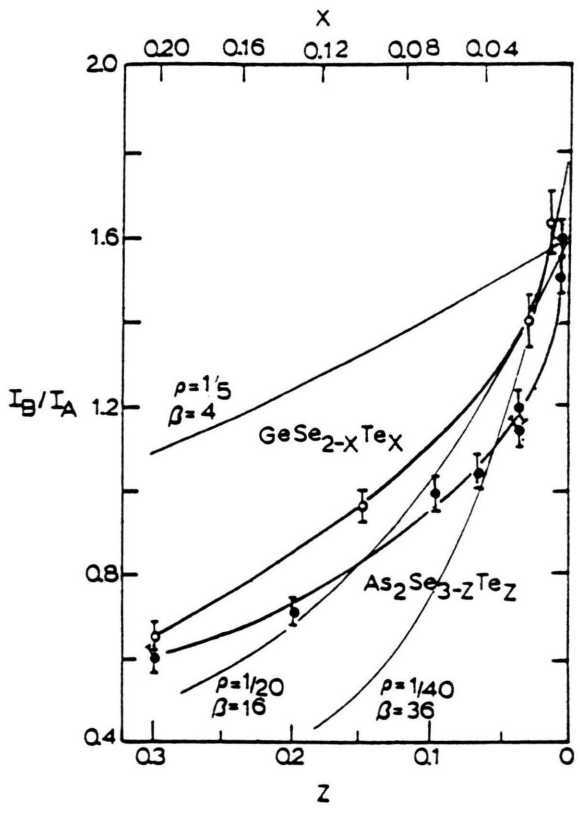

Fig. 9. Observed ^{129}I Mössbauer site-intensity ratio $I_B/I_A(z)$ variation in $As_2Se_{3-z}Te_z$ glasses (filled circles) as a function of z. Note that $I_B/I_A(z\to 0)=1.6$. The corresponding results of $GeSe_{2-x}Te_x$ glasses (open circles) is also shown for comparison. Figure taken from [40].

The concentration of chalcogen-chalcogen bonds in As_2S_3 glass networks may be larger than As_2Se_3 glass as detected by ^{125}Te and ^{129}I Mössbauer spectroscopy [41, 42]. The observed I_B/I_A ratio of 2.1 (1) in bulk $As_2S_{2.98}Te_{0.02}$ glass is found [42] to be largely independent of the melt quench temperature (T_q) in the range $500\,^\circ C < T_q < 800\,^\circ C$. The corresponding I_B/I_A ratio in bulk $As_2Se_{2.98}Te_{0.02}$ glass is found to be 1.6(1). Tentatively, if Te dopant site selectivity (β-parameter) in the S-bearing and Se-bearing glass is the same, one must conclude that the concentration of chalcogen-chalcogen bonds in the S-bearing glass is 30% higher. The β-parameter in As_2S_3 glass has not been explicitly measured yet, and for that reason one may treat the above result with care.

^{129}I Mössbauer site intensity ratios, I_B/I_A studied systematically as a function of T_q in $As_2S_{2.98}Te_{0.02}$ samples, have unexpectedly provided direct confirmation that the observable I_B/I_A closely tracks the S–S bond concentration in a glass network. At $T_q > 800\,^\circ C$, I. Zitkovsky et al. [41] have shown that the I_B/I_A ratio declines sharply to half its value at $T_q = 1000\,^\circ C$. The sharp reduction in the concentration of S–S bonds in an As_2S_3 glass sample once T_q exceeds 800 °C, i.e. when the glass is obtained by a vapor-quench instead of a melt-quench, is traced [42] to the breaking up of S_8 rings in the vapor state and thus promoting chemical ordering in the resulting glass. One consequence of this chemical ordering is a reduction in the optical band gap by about 50 meV, first reported by Tanaka [43] and subsequently confirmed by Zitkovsky [42].

The concentration of As–As bonds in a stoichiometric bulk As_2S_3 glass has been examined by a clever chemical method [44]. The results clearly reveal a finite concentration of such bonds, although the value of 5.7 mole percent of such bonds reported by Kosek et al. [44] may be on the high side. Since each As–As bond yields two chemically disordered As sites while three As–S bonds yield one chemically ordered As site, the conversion between the concentration of homopolar bonds and chemically disordered sites is a factor of 6. A 5% concentration of As–As bonds in g-As_2S_3 would thus imply a 30% concentration of chemically disordered As sites, which is actually quite high. Such a high concentration of chemically disordered As sites should be observable in ^{75}As NQR spectroscopy provided the local chemical environments of these sites are reasonably homogeneous.

Molecular Structure of Chalcohalide Glasses

The Te subhalides, Te_3X_2, where X = Cl, Br or I, have attracted interest [45] as optical materials transmitting IR radiation up to 20 μ. These materials are excellent glass formers as well, and thus are potential IR transmitting optical fiber materials. Presently little is known about the molecular structure of these glasses. These glasses are usually modelled [46] after c-Te_3Cl_2, which consists of a polymeric chain structure (Fig. 10) in which two types of the Te environments occur; site A, 2-fold coordinated to two Te nearest-neighbors (nns) and site B, 4-fold coordinate to two Te and two Cl nns in a trigonal bipyramid coordination as illustrated in Figure 10. In the infinitely long chains characterizing the crystalline phase, the ratio of the frequency of occurrence of sites A:B is 2, and the average coordination number of the

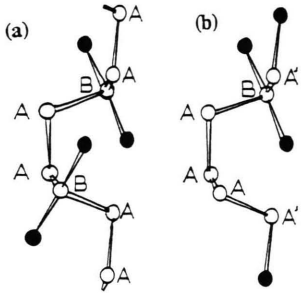

Fig. 10. (a) Polymeric chain structure of c-Te_3Cl_2 following the work of Kniep et al., [46]. (b) Proposed molecular structure of g-Te_3Cl_2 and g-Te_3Br_2 consisting of halogen terminated Te-chain fragments deduced from ^{129}I Mössbauer spectroscopy results.

chain-structure is 2. In analogy to elemental Se, the pronounced glass forming tendency of these chalcohalides probably derives from the intrinsic floppiness of such a chain structure following the ideas of constraint theory [34, 35] of glasses. Of special interest is the presence of a large concentration of one-fold coordinated halogen atoms in these glasses, which can serve for testing the role of dangling bonds in determining the mechanical properties [36] of these networks.

Mössbauer Spectroscopy Results

It would be well to recall here that in the As- and Ge-chalcogenides, Te was introduced as a dopant to probe anion-sites of these glass networks. Mössbauer spectroscopy measurements were undertaken as a function of glass composition to separate dopant site selectivity (β-parameter) from the degree of broken chemical order (ϱ-parameter) intrinsic to the glass network. In sharp contrast to those measurements, in the present chalcohalides, since Te is a natural cation present, Mössbauer spectroscopy measurements can be undertaken at the stoichiometric composition directly to elucidate the nature of glassy networks.

Such Mössbauer experiments have recently been reported [9] by J. Wells et al. on both Te_3Cl_2 and Te_3Br_2 bulk glasses. These experiments demonstrate (Fig. 11) a trimodal distribution of Te-sites (A-, B-, and A′-sites). The observed ^{129}I electric hyperfine structure ($e^2 q Q, \eta, \delta$) has served to unambiguously provide the Te-site assignments (Figure 3). Two of these sites (A and B) are characteristic of c-Te_3Cl_2 chains. Specifically, sites A is identified with a Te atom 2-fold coordinated to two Te nearest-neighbors (nns) as in an amorphous Te_n chain. Site B is identified with a Te atom four-fold coordinated to a pair of Te and a pair of Cl (or Br) nns in a pseudo trigonal bipyramidal coordination. The third site, site A′, peculiar to the glasses is identified as a Te atom 2-fold coordinated to a Te and a halogen nn. This site is thought to be a chain-terminating site. It is thought to be populated in the stoichiometric glass at the expense of an intrachain B-site transforming to an A-site and releasing a pair of halogens (Figure 10). The released halogens can serve to terminate the chain fragments in the stoichiometric glass network.

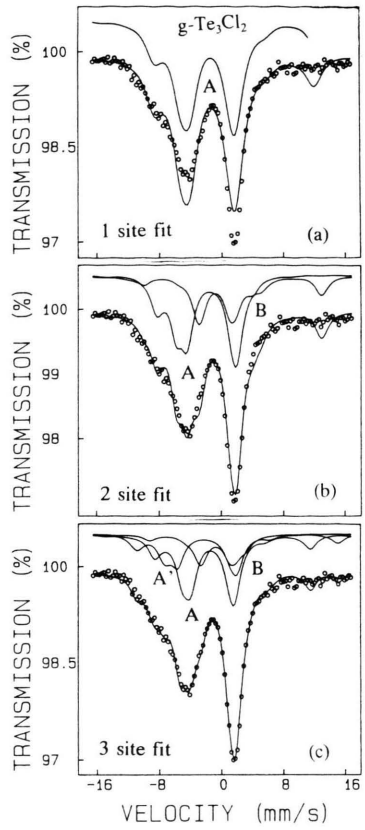

Fig. 11. ^{129}I emission spectrum of g-Te_3Cl_2 deconvoluted in terms of (a) one, (b) two, (c) three sites. Figure taken from [9].

Nuclear resonant cross-sections are independent of chemical environment. The integrated area (I) under the resonance lineshape provides a quantitative measure of the site concentrations (N), i.e. $I = Nf$, where f is the recoil-free fraction. In the chalcohalides the ob-

served site integrated intensity ratios I'_A/I_A (and also I'_A/I_B) directly reflect site concentrations N'_A/N_A (and also N'_A/N_B) provided the recoil-free-fractions $f_{A'}=f_B=f_A$. Since the ^{129}I Mössbauer spectroscopy measurements on Te_3Cl_2 and Te_3Br_2 glasses were performed at 4.2 K, it is likely that the f-factors of each of the sites are the same within 10%.

In the chain-fragment model of these chalcohalide glasses developed above, counting arguments reveal that the site concentration ratios

$$N'_A/N_A = 2/(2n-1), \tag{7}$$

$$N'_A/N_B = 2/(2n-1), \tag{8}$$

where n represents the number of Te_3Cl_2 formula units in a chain-fragment. As the chain-length gets smaller ($n \to 1$), the surface (chain-end sites) to volume (intrachain sites) ratio of a chain fragment increases. In Fig. 12, taken from [9], the two curves show a plot of these concentration ratios as a function of n, the number of formula units in a chain. For Te_3Cl_2 (and also Te_3Br_2) glass, the observed ^{129}I site intensity ratios are shown by rectangular boxes on the ordinate in this figure. One notes that the observed values of I'_A/I_B and I'_A/I_A ratios independently indicate an average chain-length $n \simeq 2$ formula units (Fig. 12), and corresponds to a length of about 1.5 nm. This average chain length corresponds to a fictive temperature of 500 °C, the temperature at which melts were equilibrated.

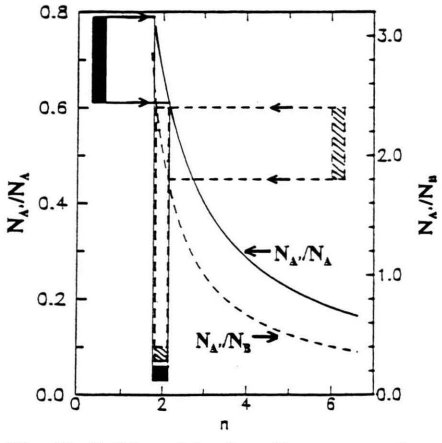

Fig. 12. Solid and broken line curves show a plot of the expected site concentration ratios N'_A/N_A and N'_A/N_B, respectively, as functions of chainlength n. n represents the number of Te_3Cl_2 formula units in the chain. The observed site-intensity ratios I'_A/I_A and I'_A/I_B for both Te_3Cl_2 and Te_3Br_2 glass fall in the rectangular boxes (filled and shaded), and each independently suggests a length of $n \simeq 2$ formula units for the chain-fragments.

These results constitute one of the first direct absolute chain-length measurement in any network glass. In Se, one of the most studied chain glass, melt viscosities have been modelled [47] to indirectly deduce relative chain-length reduction with temperature. The absolute value of Se chain-length at the melting point in these model studies is found to vary by more than four orders of magnitude, however.

Conclusions

Experimental methods such as Mössbauer spectroscopy, NQR, solid state NMR, and Raman scattering have proved to be powerful probes of local structures in network glasses. Some of these local methods using NQI have complemented scattering methods using beams of neutrons of X-rays as probes of local order in network glasses. In favorable instances, when a multi-modal distribution of cation- or anion-sites can be established using one of the local probes, and one can quantitatively discriminate surface (or edge) from interior (or volume) sites, it is then also possible to deduce elements of medium-range structure in the network by examining site-intensity ratios as a function of glass composition. In the present review we have illustrated realization of this simple idea for the case of several chalcogenide and chalcohalide glasses using the Mössbauer effect.

Acknowledgements

The review is based on work done in collaboration with several individuals over the years. Some of these include Wayne Bresser, John P. deNeufville, Ray Enzweiler, Bernard Goodman, Jeff Grothaus, Stan Hanna, Chang Suk Kim, Darl McDaniel, Jim Oberschmidt, Stan Ovshinsky, Jim Phillips, Dave Ruffolo, Mike Tenhover, Mark Stevens, Peter Suranyi, Jack Wells, Y. Wu, Min Zhang, and Ivan Zitkovsky. It is a pleasure to acknowledge their participation, interest and encouragement. This work was supported by National Science Foundation grant DMR-92-07166.

[1] S. C. Moss and D. L. Price, Physics of Disordered Solids, D. Adler, H. Fritzsche, and S. R. Ovshinsky, ed. Plenum, New York 1985, p. 77.
[2] T. P. Das and E. L. Hahn, Nuclear Quadrupole Resonance Spectroscopy, Supplement I of Solid State Physics, Academic Press, Inc., New York 1958.
[3] P. E. Stallworth and P. J. Bray in Glass Science and Technology, Vol. 48, (Academic Press, Boston 1990, p. 77) ed. D. R. Uhlman, N. J. Kreidl.
[4] P. Z. Hien, V. G. Shapiro, and V. S. Spinel, Soviet Physics – JETP **15,** 489 (1962). Also see N. Shikazono, T. Shoji, H. Takekoshi, and P. Tseng, J. Phys. Soc. Japan **17,** 1205 (1962).
[5] S. Jha, R. Segnan, and G. Lang, Phys. Rev. **128,** 1160 (1962). Although ^{129}I has a half life of 1.7×10^7 years and therefore no natural abundance, in this pioneering work it was demonstrated that an absorber of tens of milligrams of ^{129}I in a cubic host can be used to observe the effect.
[6] P. Boolchand, Mössbauer Spectroscopy – a Rewarding Probe of Morphological Structure of Network Glasses, in Amorphous Materials Devices, Vol. I, D. Adler, B. B. Schwartz, and M. C. Steele, Plenum, New York 1985, p. 221.
[7] W. J. Bresser, M. Zhang, L. Koudelka, J. Wells, P. Boolchand, G. J. Ehrhart, and P. Miller, Phys. Rev. **B47,** 11663 (1993).
[8] W. J. Bresser, P. Boolchand, P. Suranyi, and J. P. deNeufville, Phys. Rev. Lett. **46,** 1689 (1981); W. Bresser, Ph.D. thesis, Univ. of Cincinnati (unpublished) 1989.
[9] J. Wells, W. J. Bresser, P. Boolchand, and J. Lucas, J. Non. Cryst. Solids (in press).
[10] G. Langouche, B. B. Triplett, N. S. Dixon, Y. Mahmud, and S. S. Hanna, Phys. Rev. **B15,** 2504 (1977) and references therein.
[11] P. Boolchand, B. L. Robinson, and S. Jha, Phys. Rev. **B12,** 3463 (1970).
[12] H. deWaard in Mössbauer effect data index 1973, ed. by J. G. Stevens and V. E. Stevens, Plenum, New York 1975, p. 447, and references therein.
[13] C. S. Kim and P. Boolchand, Phys. Rev. **B19,** 3187 (1979).
[14] C. H. Townes and B. P. Daily, J. Chem. Phys. **17,** 782 (1949).
[15] R. G. Barnes and W. V. Smith, Phys. Rev. **93,** 95 (1954).
[16] T. P. Das (private communication).
[17] H. Sakai, J. Sci. Hiroshima Univ. Ser **A36,** 47 (1972); also see J. Trotter and T. Zobel, Z. Krist. **123,** 67 (1966).
[18] J. L. Warren, C. H. W. Jones, and P. Vasudev, J. of Phys. Chemistry **75,** 2867 (1971); also see S. L. Ruby and G. K. Shenoy, Phys. Rev. **186,** 326 (1969).
[19] E. A. Porai Koshits in: Glass Science and Technology, Vol. 4A ed. D. R. Uhlmann and N. J. Kreidl, Academic Press, Boston, MA 1990, p. 1.
[20] For a review see G. N. Greaves in Glass Science and Technology, Vol. 4B, Academic Press, Inc., Academic Press, Inc. Boston, MA 1990, p. 1–76.
[21] M. Rubinstein and P. C. Taylor, Phys. Rev. **B9,** 4258 (1974); also see D. J. Treacy, U. Strom, P. B. Klein, P. C. Taylor, and T. P. Martin, J. Non-Cryst. Solids **35** and **36,** 1035 (1980).
[22] G. Lucovsky, F. Galeener, R. C. Keezer, R. H. Geils, and H. A. Six, Phys. Rev **B10,** 5134 (1974).
[23] K. Murase, T. Fukanaga, Y. Tanaka, K. Yakushiji, and I. Yunoki, Physica **117B** and **118B,** 962 (1983).
[24] P. Vashishta, R. K. Kalia, and I. Ebbsjö, Phys. Rev. **B39,** 6034 (1989); also see Phys. Rev. Lett. **62,** 1651 (1989).
[25] M. B. Meyers and E. J. Felty, Mat. Res. Bull. **2,** 535 (1967), D. J. Sarrach, J. P. deNeufville, and W. L. Haworth, J. Non. Cryst. Solids **22,** 245 (1976).
[26] V. G. Dittmar and H. Schäfer, Acta Cryst. **832,** 2726 (1976).
[27] N. Morimoto, Mineral J. (Sappore) **1,** 160 (1954).
[28] W. H. Zachariasen, J. Amer. Chem. Soc. **54,** 3841.
[29] P. M. Bridenbaugh, G. P. Espinosa, J. E. Griffith, J. C. Phillips, and J. P. Reneika, Phys. Rev. **B20,** 4140 (1979).
[30] J. C. Phillips, C. Arnold Beevers, and E. B. Gould, Phys. Rev. **B21,** 5724 (1980).
[31] P. Boolchand, J. Grothaus, W. J. Bresser, and P. Suranyi, Phys. Rev. **B25,** 2975 (1982).
[32] K. Murase, K. Inoye, and O. Matsuda, in Current Topics in Amorphous Materials: Physics and Technology, ed. Y. Sakurai, Y. Hamakana, T. Masumoto, K. Shirane, and K. Suzuki, Elsevier, Amsterdam 1993, p. 47.
[33] I. T. Penfold and P. S. Salmon, Phys. Rev. Lett. **67,** 97 (1991); also see P. Boolchand and J. C. Phillips, Phys. Rev. Lett. **68,** 252 (1992) and I. T. Penfold and P. S. Salmon, Phys. Rev. Lett. **68,** 253 (1992).
[34] J. C. Phillips, J. Non. Cryst. Solids **34,** 153 (1979) and ibid **43,** 37 (1981).
[35] M. F. Thorpe, J. Non. Cryst. Solids **57,** 355 (1983).
[36] P. Boolchand and M. F. Thorpe, Phys. Rev. **B50,** 10366 (1994).
[37] R. Zallen, M. L. Slade, and A. T. Ward, Phys. Rev. **B3,** 4257 (1971); R. J. Koblinska and S. A. Solin, Phys. Rev. **B8,** 756 (1973), R. J. Nemanich, G. A. Connell, J. H. Hayes, and R. A. Street, Phys. Rev. **B18,** 6900 (1978).
[38] J. Szeftel and H. Alloul, Phys. Rev. Lett. **42,** 1691 (1978); also see J. Szeftel, Phil. Mag. **B43,** 549 (1981).
[39] J. Wells and P. Boolchand, J. Non. Cryst. Solids **89,** 31 (1987).
[40] P. Suranyi, W. Bresser, J. Wells, and P. Boolchand (unpublished); also see P. Boolchand, W. J. Bresser, and P. Suranyi, Hyp. Int. **27,** 385 (1986).
[41] I. Zitkovsky and P. Boolchand, in Diffusion and Defect Data, 53–54, 167 (1987).
[42] I. Zitkovsky, Ph.D. Thesis (unpublished), Univ. of Cincinnati 1989.
[43] K. Tanaka, S. Gohda, and A. Odajima, Solid State Commun. **56,** 899 (1985).
[44] F. Kosek, J. Chlebny, Z. Cimpl and J. Masek, Phil. Mag. **B47,** 627 (1983).
[45] J. Lucas, Solid State Ionics **39,** 105 (1990).
[46] R. Kniep, D. Mootz, and A. Rabenau, Angew. Chem. International ed. **12,** 499 (1973).
[47] W. C. Cooper and R. A. Westburg, in Selenium, Van Nostrand Reinhold Co., 1974, p. 108, ed. R. A. Zingaro and W. Cooper.